Nanowires

Large-Scale Production of NbS_2 Nanowires and Their Performance in Electronic Field Emission**

Yi Zheng Jin, Wen Kuang Hsu, Yu Lun Chueh, Li Jen Chou, Yan Qiu Zhu, Kieren Brigatti, Harold W. Kroto, and David R. M. Walton*

In addition to carbon nanotubes, the production of noncarbon nanostructures has attracted much attention over the past few years. In particular, and due to their unusual geometry and promising physical properties, inorganic fullerene nanostructures have become one of the main focuses in nanoscale research since the first report of the synthesis of WS_2 nanotubes in 1992.[1] The synthesis of chalcogenide nanotubes and nested nanoparticles is difficult because their formation requires the release of considerable strain energy against

[*] Dr. Y. Q. Zhu
School of Mechanical, Materials and Manufacturing Engineering
University of Nottingham, University Park NG7 2RD (UK)
Fax: (+44) 115-951-3800
E-mail: yanqiu.zhu@nottingham.ac.uk
Y. Z. Jin, K. Brigatti, Prof. H. W. Kroto, Dr. D. R. M. Walton
Department of Chemistry, University of Sussex
Brighton BN1 9QJ (UK)
Dr. W. K. Hsu, Dr. Y. L. Chueh, Dr. L. J. Chou
Department of Materials Science and Engineering
National Tsing-Hua University
Hsinchu 300 (Taiwan)

[**] We thank the EPSRC (UK), UST-CNST of the National Tsing-Hua University, and the National Science Council (Taiwan, NSC92-2119M-007-072) for financial support.

  DOI: 10.1002/ange.200460447

surface curvature and wall thickness.[2] These chalocogenides (MX_2: M = W, Mo, Ta, Nb; X = S, Se) are mostly triple-layer structures in which one M and two S atoms are organized within a trigonal prismatic lattice. The formation of curved MX_2 morphologies commonly involves a considerable number of lattice defects and dislocations.[3,4] It has been shown, for example, that defect-containing WS_2 lattices lead to branched layer structures, which fuse particles together.[5] Lattice dislocations also provide connecting sites with C and Mo to form heterogeneous structures.[6] Recently, NbS_2 nanostructures have been produced by heating NbS_3 in the presence of H_2,[7] by the reaction between $NbCl_4$ and H_2S,[8] and by taking advantage of the carbon nanotube template effect.[9] However, the amounts of resulting materials are minute, and thus their chemical and physical properties and applications cannot be explored.

Herein we report that well-defined NbS_2 nanowires can be generated in bulk by direct heating of Nb and S powders in sealed quartz tubes in the presence of I_2. The large quantity of NbS_2 nanowires produced allows various analyses, including X-ray diffraction (XRD), the use of a superconducting quantum interference device (SQUID), and for the first time, electronic field emission tests to be performed.

In a typical experiment, Nb powder (99.8%, 325 mesh, Aldrich Co.), S powder (99.98%, Aldrich Co.), and I_2 (99.999%, Aldrich. Co) were used. A mixture of Nb and S powder with a Nb/S ratio of 1:2 was sealed in an I_2-containing quartz ampoule (ca. 2 mg cm^{-3}) under vacuum (ca. 10^{-4} pa); the I_2 is the reaction medium.[10] The ampoule was heated in either a temperature gradient (10 K cm^{-1}; 600–800 °C) three-zone horizontal furnace or at a constant temperature of 800 °C in a conventional horizontal furnace, for three days. The quartz ampoule was then allowed to cool to room temperature and the sample was subsequently extracted from the tube (colder tube end for those samples heated in a temperature gradient), washed with CS_2, and dried under vacuum. The resulting samples (200–500 mg) were then examined by XRD (Siemens, D5000), scanning electron microscopy (SEM, LEO5000), transmission electron microscopy (TEM, H7100) and high-resolution transmission electron microscopy (HRTEM, JEOL-3000), energy dispersive X-ray (EDX) line-scan, electron diffraction (ED), SQUID magnetometry, and field emission analyses. To identify the I_2 mediation effect, experiments were also carried out in the absence of I_2.

Figure 1a shows an SEM image recorded from the transported materials found at the colder end of an ampoule heated in a temperature gradient. The product consists of almost pure one-dimensional (1D) nanostructures with diameters in the range 50 to 500 nm. Experiments carried out at a constant temperature (800 °C) also generated a bulk yield of nanowires (inset, Figure 1a). Most of these nanowires have diameters within the range 20 to 200 nm, much smaller than those shown in Figure 1a. The lengths of the nanowires are typically several micrometers; wires longer than 10 μm were also observed in our TEM investigations (Figure 1b). The aspect ratio of the nanowires was estimated to be about 80–120, lower than the typical range for carbon nanotubes (150–200). The surface of the nanowires is generally clean, although a few particles were occasionally observed attached to the

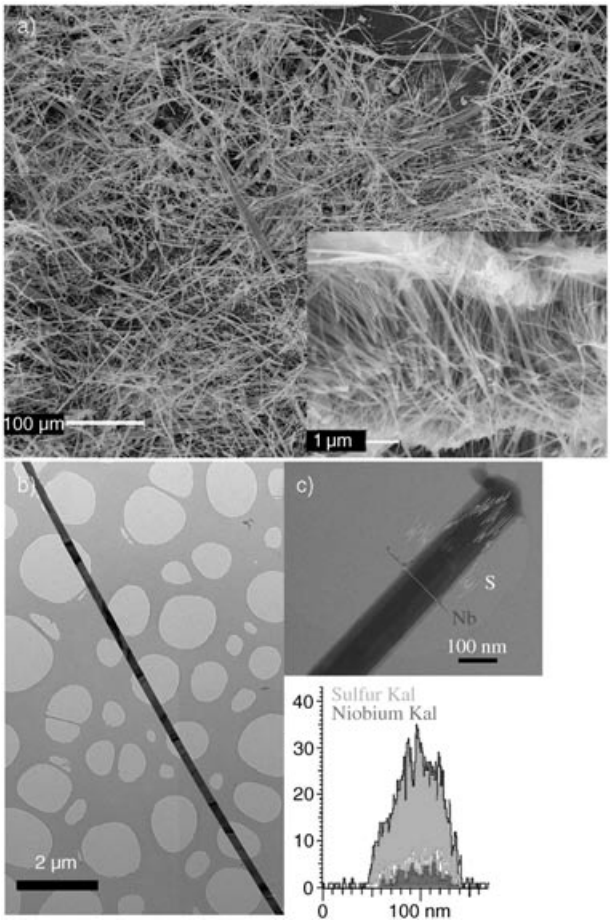

Figure 1. a) SEM image of NbS_2 nanowires from the colder end of an ampoule heated in a temperature gradient. Insert: nanowires from the constant-temperature heating; b) TEM image of a long NbS_2 nanowire (>10μm); c) line-scan EDX profile across a nanowire. Lower insert: enhanced EDX profile.

nanowire surfaces by SEM. No nanowires were produced in the I_2-free experiments; microsized crystallites and amorphous materials appeared to be the main products. These results clearly indicate that I_2-mediation is essential for the nanowire growth; this conclusion is consistent with previous results.[10]

The following studies focus on the product obtained from experiments carried out at a constant temperature, as this procedure also yields bulk materials and the diameters of the resultant nanowires are smaller than those shown in Figure 1a. Line-scan EDX analyses were carried out on selected wires. A typical elemental profile is displayed in Figure 1c; Nb and S were detected in most cases. It is noteworthy that a weak I signal is also present occasionally in the EDX profiles. We were unable to determine the exact Nb/S atomic ratio as the energy counts were only calculated based on the K_{a1} shells.

According to a commonly used inorganic crystal structure data (ICSD) file for modeling structures based on the atomic positions, the nanowire samples fit the 3*R* structure quite well. Figure 2a shows simulated XRD profiles of hexagonal-2*H* (top) and -3*R* (middle) structures based on ICSD data, along

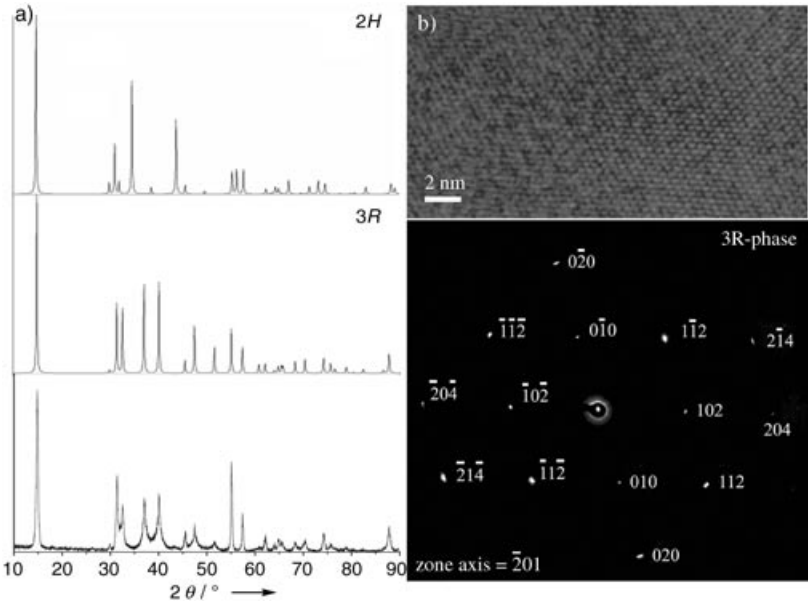

Figure 2. a) Simulated 2*H*(top) and 3*R* (middle) as well as experimental (bottom) XRD profiles; b) HRTEM image of one NbS_2 nanowire (top) and its corresponding ED pattern (bottom).

with the experimental XRD pattern (bottom). It is clear that the sample is in good agreement with the 3*R* phase, including the peak positions and intensities. The ED pattern obtained from selected wires also suggests a 3*R* phase (Figure 2b); the high-resolution TEM image clearly demonstrates the well-crystallized single-crystal structures of the NbS_2 nanowires (top right).

According to the XRD and ED analyses it seems that the presence of trace amounts of I in the NbS_2 nanowires does not alter the 3*R* structure significantly. It is possible that I substitutes S, leading to an intact 3*R*-phase lattice.

Our SQUID measurements were carried out between 300 and 2 K; no Curie temperature (T_c) was observed (Figure 3). The profile shows a positive (paramagnetic) but weak temperature dependence of the magnetic susceptibility (χ), which is consistent with 3*R*-NbS_2 (Pauli behavior).[11] A clear Curie tail is present below 20 K, thus indicating a possible high density of electronic impurities in the nanowires. In addition to the residual I, these impurities could also arise from nonstoichiometric NbS_2 phases, such as $Nb_{1+x}S_2$. This assumption is based on a previous report that starting materials with a 1:2 (Nb/S) ratio always lead to $Nb_{1+x}S_2$ phases.[12]

The field-emission behavior of NbS_2 nanotubes is well-defined, although they have a lower aspect ratio than carbon nanotubes. Figure 4a shows the results of repeating field emission tests over four runs with a similar emitting current (5 $\mu A\,cm^{-2}$) and threshold field (5.5 $V\,\mu m^{-1}$). The emitting current and threshold field of carbon nanotubes often vary from sample to sample (0.3 $\mu A\,cm^{-2}$–0.7 $A\,cm^{-2}$), due to the C-layer oxidation lattice defects.[12–14] The similar current density and turn-on voltage of our sample over several runs indicate that highly stable electronic field emission from NbS_2 nanowires is achieved via a unique energy state. The saturation current obtained here (5 $\mu A\,cm^{-2}$, Figure 4a) is much lower than that of the carbon nanotube films reported recently (0.7 $A\,cm^{-2}$),[14] but is similar to that of annealed single-walled carbon nanotubes (0.5–5 $\mu A\,cm^{-2}$).[15] This phenomenon supports our assumption that the electrons only emit by a specific channel, possibly the d_{z^2}-band. In this respect the lower current density obtained with our nanowire sample is not disappointing because a single emission channel will certainly limit the current density. The larger emitting current density seen in

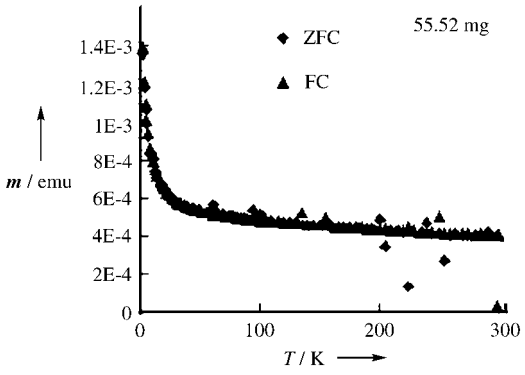

Figure 3. SQUID profile of 3*R*-NbS_2 nanowires. ***m*** is the magnetic moment.

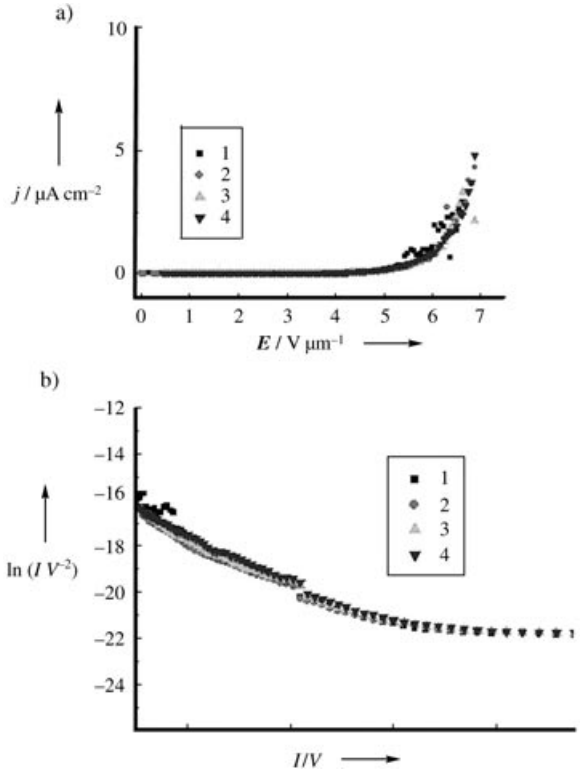

Figure 4. Electron field emission profile of NbS_2 nanowires (a), and their corresponding F–N plots (b). The numbers denote the run of the experiment. *j* is the current density; ***E*** is the electric field strength.

carbon nanotubes (particularly in multi-walled tubes) is mainly due to a high density of localized states. In other words, electrons can emit by various channels at the tube tips or elsewhere.[16] However, the multiple emission channels in multiwalled carbon nanotubes are unstable: the field emission from point defects, for example, can be rapidly quenched by joule heating, and other localized spinless defects can be electronically reopened. This explains the frequent changes of field emission current from carbon nanotubes over repeated experiments. The low current density from single-walled carbon nanotubes is also due to a similar situation, that is, a lower density of localized emitting channels. Our NbS_2 nanowires show a linear Fowler–Nordheim (F–N) plot at high field (Figure 4b), whereas the F–N profile becomes nonlinear at low field (Figure 4b). The turn-on voltage determined from the F–N plot is about 2.5 $V\,\mu m^{-1}$. This value is similar to that in carbon nanotubes (CNTs) but is significantly lower than other metal oxide and inorganic nanostructures. Repeating the experiments yielded similar results (1st to 4th run, Figure 4). To highlight the performance of NbS_2 nanowire emitters, various metal oxide and inorganic nanowire emitters are listed below along with their threshold fields: Co nanowire arrays (14 $V\,\mu m^{-}$),[17] MoS_2 nanoflowers (ca. 8 $V\,\mu m^{-}$),[18] SiC nanorods (ca. 15 $V\,\mu m^{-}$),[19] $W_{18}O_{49}$ nanowire films (6.2 $V\,\mu m^{-}$),[20] and ZnO nanorods (6 $V\,\mu m^{-}$).[21]

The presence of a discontinuity in the F–N plot (arrow, Figure 4b) is due to the switching of the emission control circuits from lower (nA magnitude) to higher power (μA magnitude). Small deviations in the F–N plot often occur in carbon nanotube emission due to various factors, including screening, space charge, and variation in the emission states. A small curve that appears in the lower-field region of the F–N plot (Figure 4b) can be attributed to a new factor, namely the surface amorphous structure (Figure 5a,b). The surface amorphous material also consists of Nb and S, as revealed by EDX. HRTEM shows two kinds of order–disorder phase transitions near to the wire surfaces: (a) a gradual lattice variation (Figure 5a), and (b) a coating-like structure (Figure 5b). The former is a distinguishable structural transition from ordered to disordered, (arrow, Figure 5a), whereas the latter is a thicker amorphous structure (Figure 5b). The disordered surface structure is likely to be the nonstoichiometric NbS_2 phase, which appears as a result of the chemical changes in the reaction environment with time. A strong electron scattering is anticipated at the surface amorphous layers. The scattering, in turn, influences the field emission properties, including the emission current and applied threshold field. Meanwhile, the amorphous NbS_2 layers may be gradually converted into a stable oxide phase (Nb_2O_5); consequently, the lifetime of field emission shortens.

In summary, a large quantity of quality NbS_2 nanowires (hundreds of milligrams) has been produced successfully by direct heating of Nb and S powders in the presence of I_2 at 800 °C. This synthetic route is novel and straightforward. The materials have a 3*R* phase and are metallic in nature. Repeating field emission tests revealed that the NbS_2 nanowires are highly reliable field emitters and exhibit a very low turn-on voltage, which is among the best amongst inorganic 1D nanomaterials and is comparable with those of carbon nanotubes.

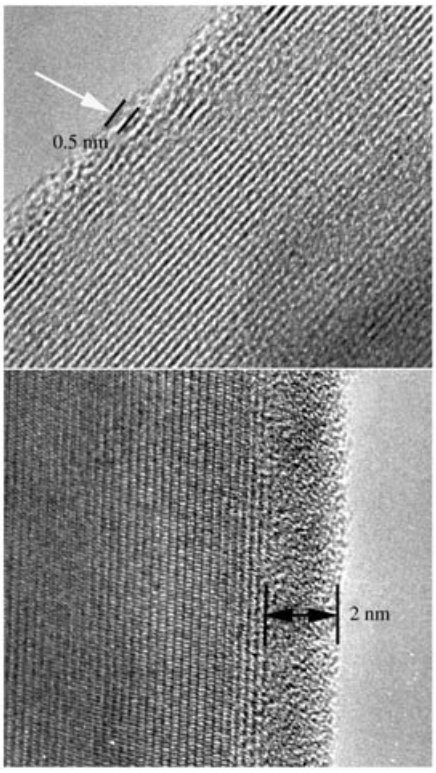

Figure 5. HRTEM images: a) a thin amorphous layer structure near to the nanowire surface at about 0.5 nm (arrowed). b) a thick coating-like amorphous structure on the wire surface at about 2 nm (arrowed).

Received: April 26, 2004

Keywords: nanostructures · niobium · sulfur

[1] R. Tenne, L. Margulis, M. Genut, G. Hodes, *Nature* **1992**, *360*, 444.
[2] D. J. Srolovitz, S. A. Safran, M. Homyonfer, R. Tenne, *Phys. Rev. Lett.*. **1995**, *74*, 1779.
[3] Y. D. Li, X. L. Li, R. R. He, J. Zhu, Z. X. Deng, *J. Am. Chem. Soc.*. **2002**, *124*, 1411.
[4] R. L. D. Whitby, W. K. Hsu, T. H. Lee, C. B. Boothroyd, H. W. Kroto, D. R. M. Walton, *Chem. Phys. Lett.*. **2002**, *359*, 68.
[5] W. K. Hsu, Y. Q. Zhu, S. Firth, M. Terrones, H. Terrones, S. Trasobares, R. J. H. Clark, H. W. Kroto, D. R. M. Walton, *Carbon* **2001**, *39*, 1107.
[6] W. K. Hsu, Y. Q. Zhu, C. B. Boothroyd, I. Kinloch, S. Trasobares, H. Terrones, N. Grobert, M. Terrones, R. Escudero, G. Z. Chen, C. Colliex, A. H. Windle, D. J. Fray, H. W. Kroto, D. R. M. Walton, *Chem. Mater.* **2000**, *12*, 3541.
[7] M. Nath, C. N. R. Rao, *J. Am. Chem. Soc.* **2001**, *123*, 4841.
[8] C. Schuffenhauer, R. Popovitz-Biro, R. Tenne, *J. Mater. Chem.*. **2002**, *12*, 1587.
[9] Y. Q. Zhu, W. K. Hsu, H. W. Kroto, D. R. M. Walton, *Chem. Commun.* **2001**, 2184.
[10] M. Remskar, A. Mrzel, Z. Skraba, A. Jesih, M. Ceh, J. Demsar, P. Stadelmann, F. Levy, D. Mihailovic, *Science* **2001**, *292*, 479.
[11] W. G. Fisher, M. J. Sienko, *Inorg. Chem.* **1980**, *19*, 39.
[12] W. A. Deheer, A. Chatelain, D. Ugarte, *Science* **1995**, *270*, 1179.

[13] G. Pirio, P. Legagneux, D. Pribat, K. B. K. Teo, M. Chhowalla, G. A. J. Amaratunga, W. I. Milne, *Nanotechnology* **2002**, *13*, 1.
[14] W. I. Milne, K. B. K. Teo, G. A. J. Amaratunga, P. Legagneux, L. Gangloff, J. P. Schnell, V. Semet, V. Thien Binh, O. Groening, *J. Mater. Chem.* **2004**, *14*, 933.
[15] J. P. Sun, Z. X. Zhang, S. M. Hou, G. M. Zhang, Z. N. Gu, X. Y. Zhao, W. M. Liu, Z. Q. Xue, *Appl. Phys. A* **2002**, *75*, 479.
[16] D. Lovall, M. Buss, E. Graugnard, R. P. Andres, R. Reifenberger, *Phys. Rev. B* **2000**, *61*, 5683.
[17] L. Vila, P. Vincent, L. Dauginet-De Pra, G. Pirio, E. Minoux, L. Gangloff, S. Demoustier-Champagne, N. Sarazin, E. Ferain, R. Legras, L. Piraux, P. Legagneux, *Nano Lett.* **2004**, *4*, 521.
[18] Y. B. Li, Y. Bando, D. Golberg, *Appl. Phys. Lett.* **2003**, *82*, 1962.
[19] X. T. Zhou, H. L. Lai, H. Y. Peng, F. C. K. Au, L. S. Liao, N. Wang, I. Bello, C. S. Lee, S. T. Lee, *Chem. Phys. Lett.* **2000**, *318*, 58.
[20] Y. B. Li, Y. Bando, D. Golberg, *Adv. Mater.* **2003**, *15*, 1294.
[21] C. J. Lee, T. J. Lee, S. C. Lyu, Y. Zhang, H. Ruh, H. J. Lee, *Appl. Phys. Lett.* **2002**, *81*, 3648.